Electronic Supplementary Material (ESI) for Journal of Materials Chemistry A.

Supporting Information

Nanostructured NiFe (Oxy)hydroxide with Easily Oxidized Ni Towards Efficient Oxygen Evolution Reaction

Dazhong Zhong[1],[a,b] Lei Zhang[1],[a] Chengcheng Li,[a] Dandan Li,[b] Congcong Wei,[b] Qiang Zhao,[b] Jinping Li*,[b] and Jinlong Gong*[a]

[a] Key Laboratory for Green Chemical Technology of Ministry of Education, School of Chemical Engineering and Technology, Tianjin University; Collaborative Innovation Center of Chemical Science and Engineering (Tianjin), Tianjin 300072, P.R. China.

[b] Research Institute of Special Chemicals, Taiyuan University of Technology, Taiyuan 030024, Shanxi, P.R. China; Shanxi Key Laboratory of Gas Energy Efficient and Clean Utilization, Taiyuan 030024, Shanxi, P.R. China.

*Corresponding author: jpli211@hotmail.com; jlgong@tju.edu.cn

1 These two authors contributed equally to this work.

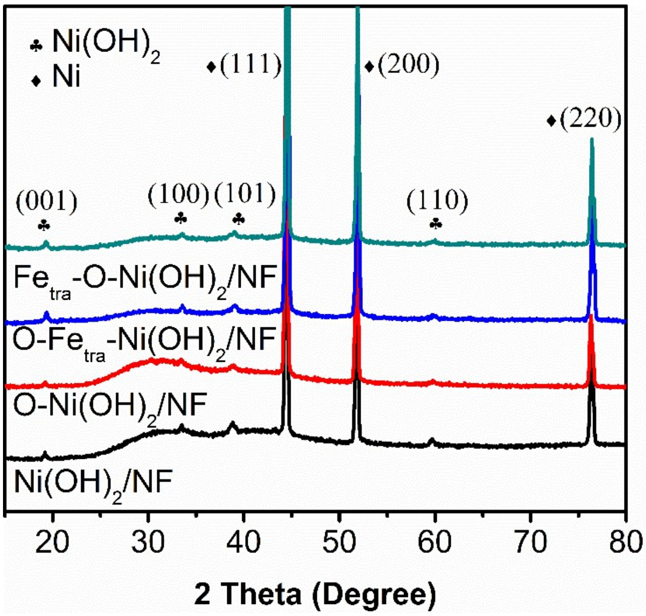

Figure S1. XRD patterns of $Ni(OH)_2$/NF, O-$Ni(OH)_2$/NF, O-Fe_{tra}-$Ni(OH)_2$/NF and Fe_{tra}-O-$Ni(OH)_2$/NF.

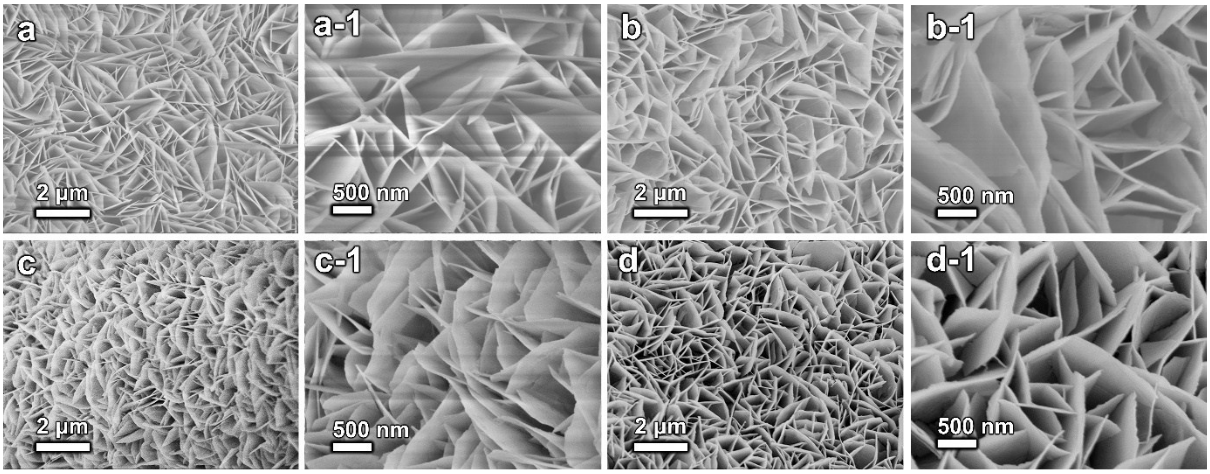

Figure S2. The SEM images of a, a-1) $Ni(OH)_2$/NF; b, b-1) O-$Ni(OH)_2$/NF ; c, c-1) O-Fe_{tra}-$Ni(OH)_2$/NF and d, d-1) Fe_{tra}-O-$Ni(OH)_2$/NF.

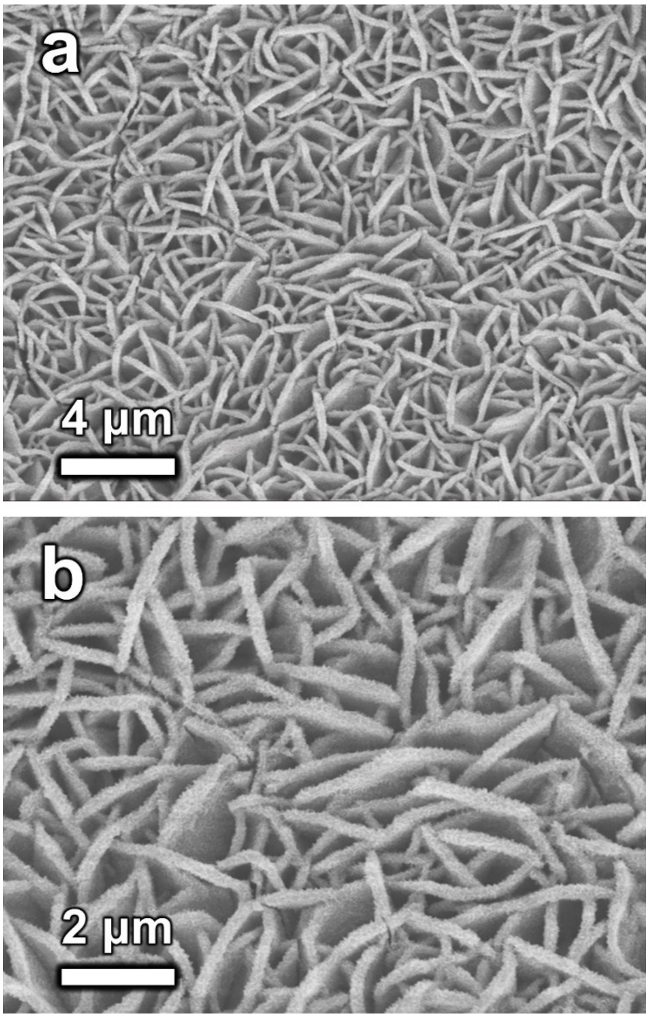

Figure S3. SEM images of Fe-O-$Ni(OH)_2$/NF.

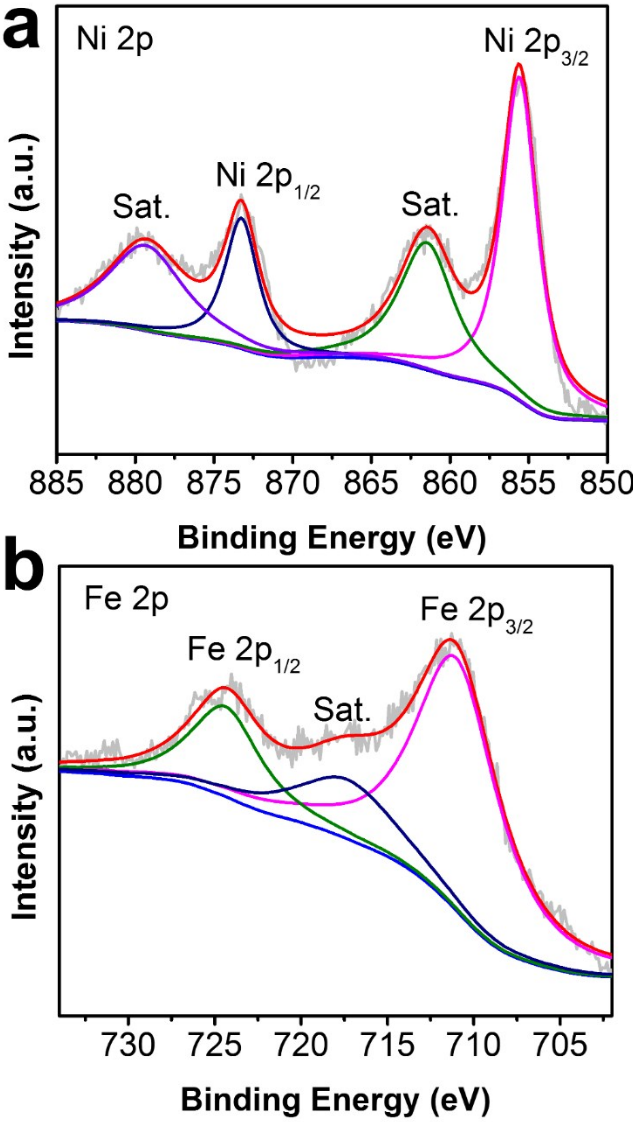

Figure S4. a) Ni 2p and b) Fe 2p spectra of Fe-O-$Ni(OH)_2$/NF.

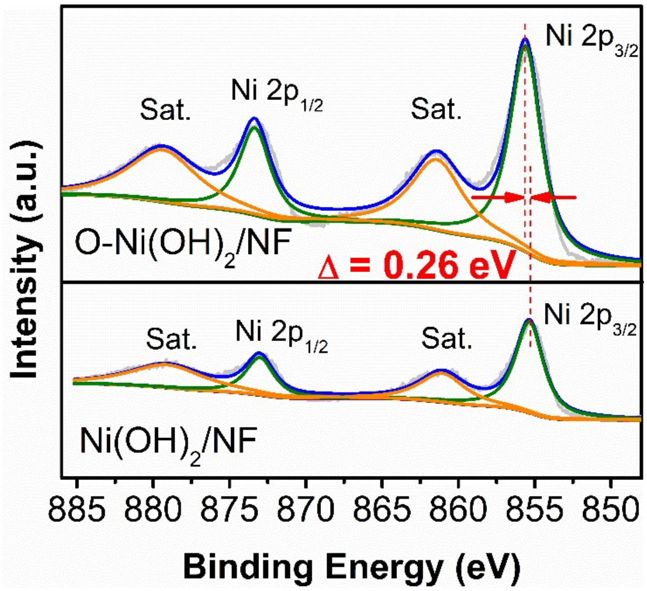

Figure S5. a) Ni 2p spectra of O-Ni(OH)$_2$/NF and Ni(OH)$_2$/NF.

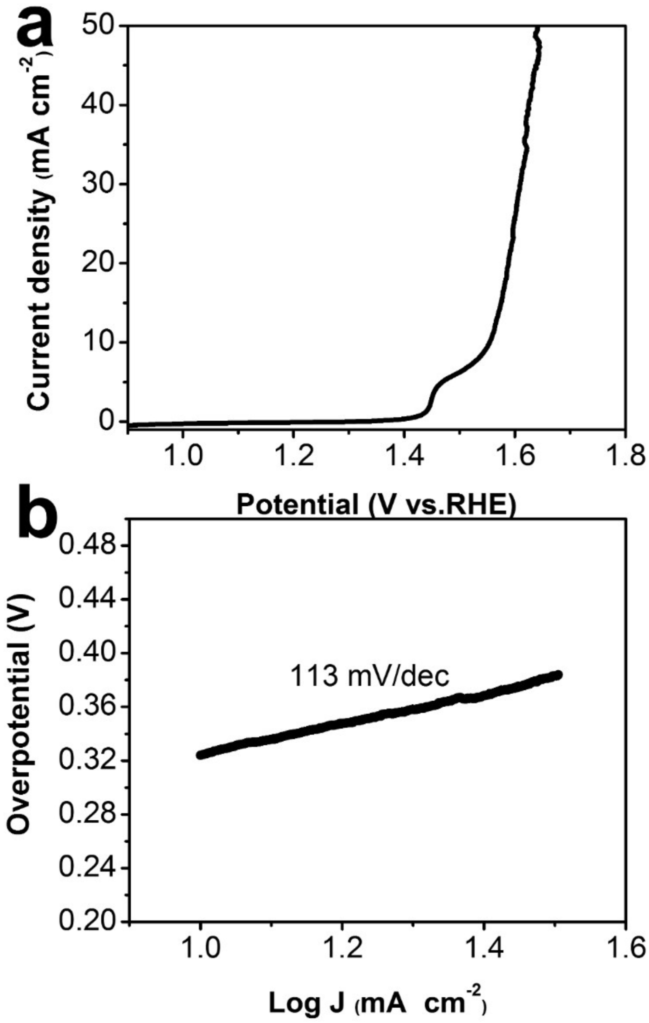

Figure S6. a) LSV cure and the correspond b) Tafel plot of Fe-O-Ni$(OH)_2$/NF with a scan rate of 2 mV s^{-1} in 0.1 M $K_2B_4O_7$ aqueous solution.

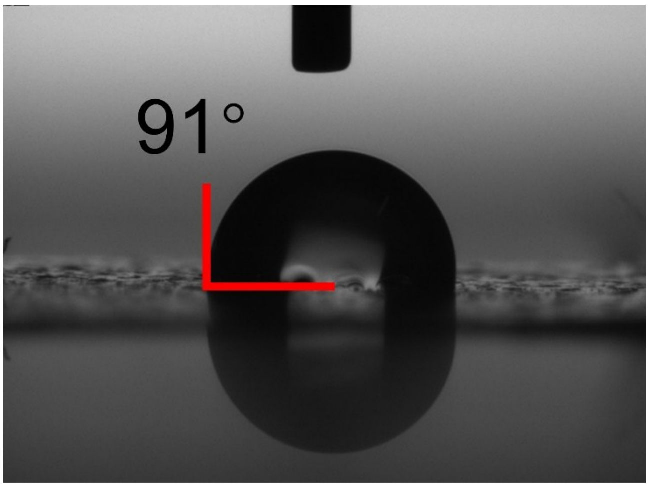

Figure S7. Contact angle images of $Ni(OH)_2$/NF.

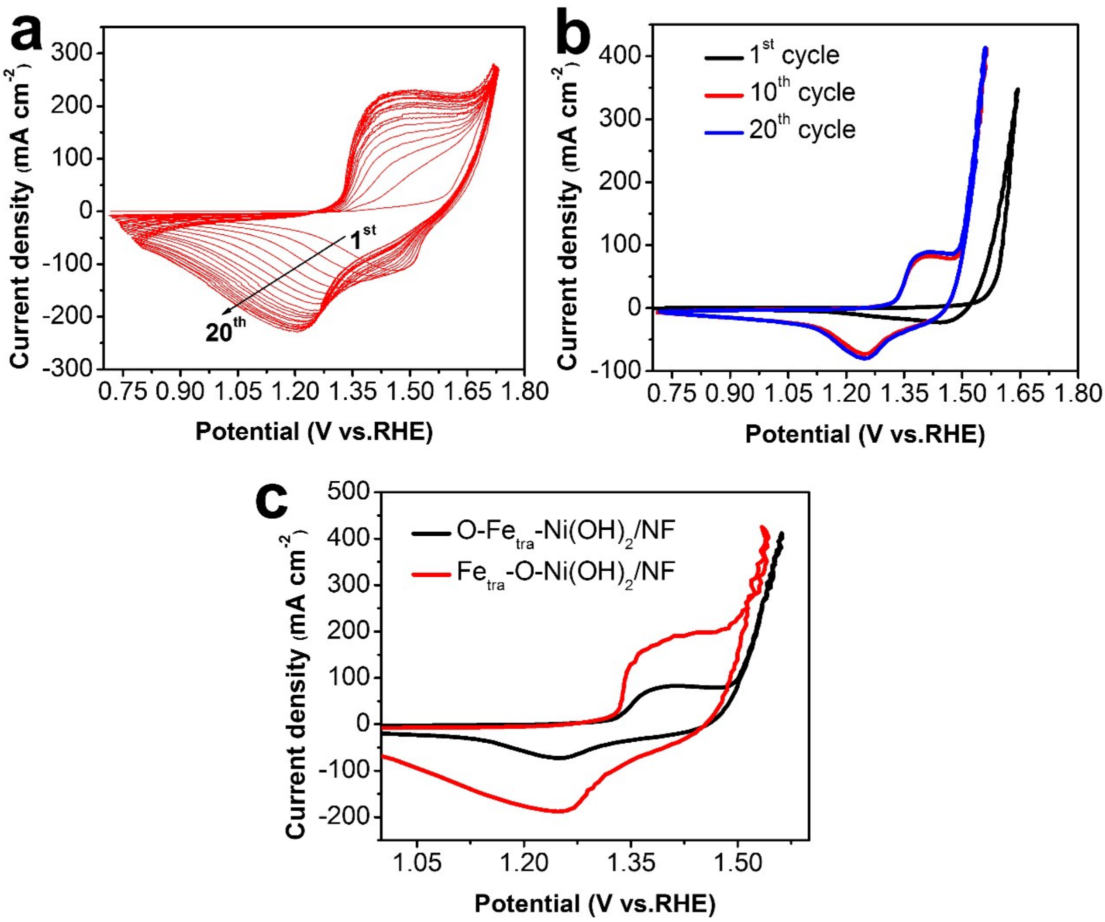

Figure S8. CV curves of the transformation process from $Ni(OH)_2$/NF to a) O-$Ni(OH)_2$/NF in 1 M Fe-free KOH and b) O-Fe_{tra}-$Ni(OH)_2$/NF in 1M Fe-containing KOH, respectively. c) The comparison of CV curves between Fe_{tra}-O-$Ni(OH)_2$/NF and O-Fe_{tra}-$Ni(OH)_2$/NF.

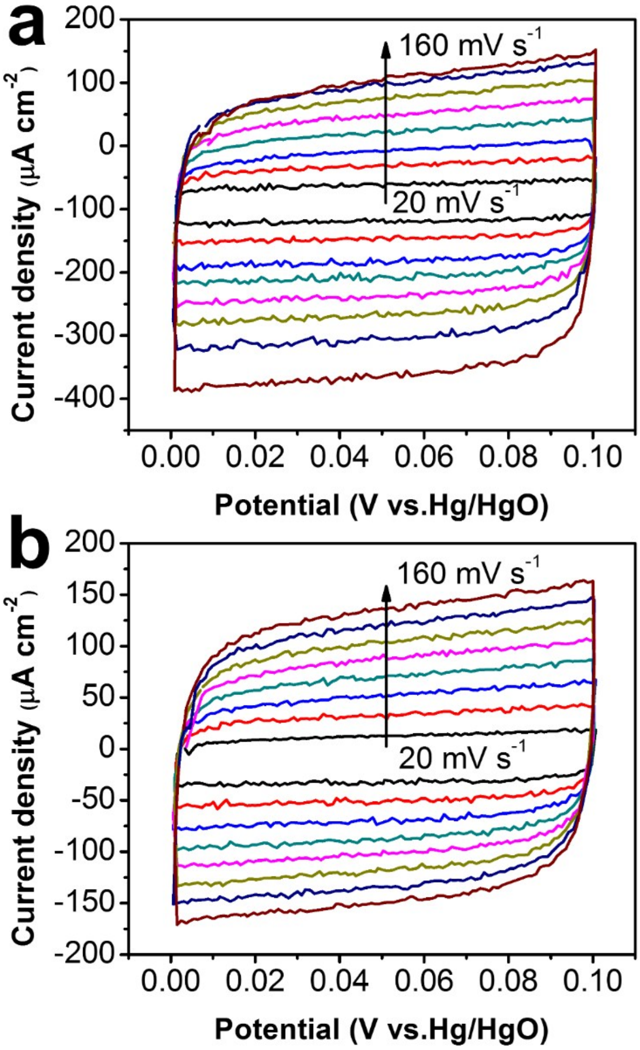

Figure S9. CV curves of a) Fe_{tra}-O-$Ni(OH)_2$/NF and b) O-Fe_{tra}-$Ni(OH)_2$/NF at the voltage between 0 and 0.1 V vs.Hg/HgO with different scan rates.

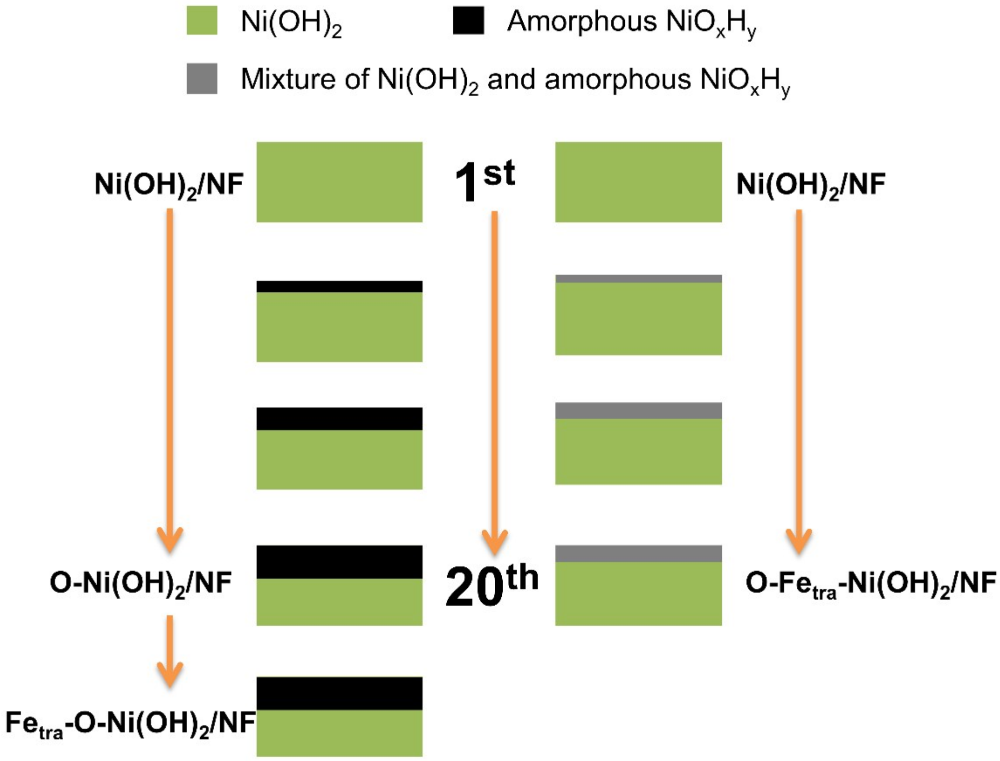

Scheme S1. The process for the formation of amorphous species during cyclic voltammetry.

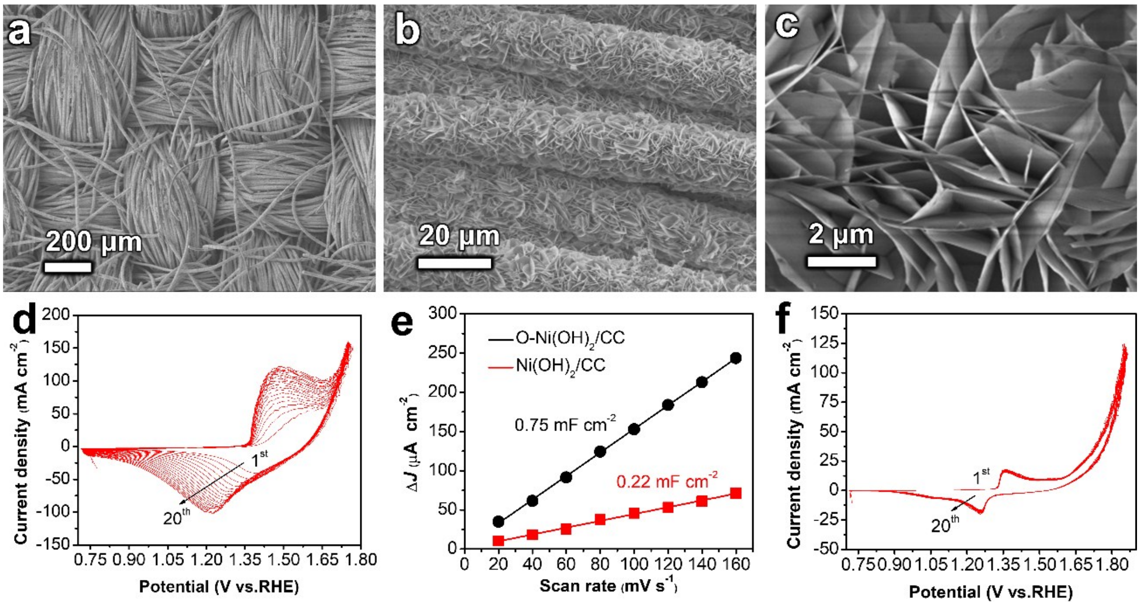

Figure S10. a-c) SEM images of $Ni(OH)_2$/CC. d) CV curve of the transformation process from $Ni(OH)_2$/CC to O-$Ni(OH)_2$/NF in 1 M Fe-free KOH. e) double-layer capacitance (Cdl) for the representation of ECSA. f) CV curve of the transformation process of blank Ni foam in 1 M Fe-free KOH

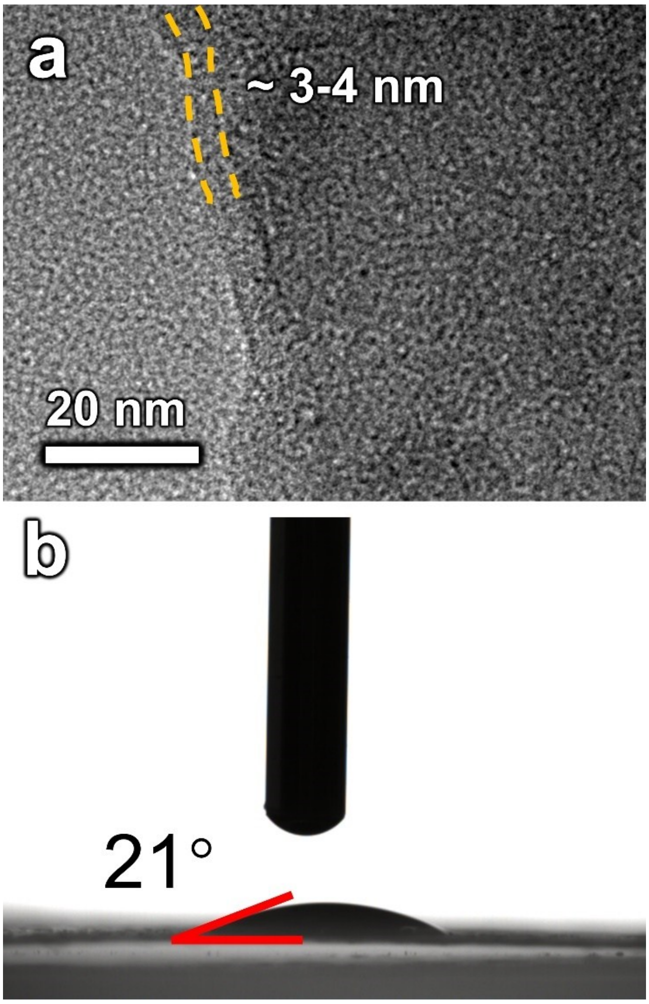

Figure S11. a) TEM and b) contact angle images of O-$Ni(OH)_2$/NF.

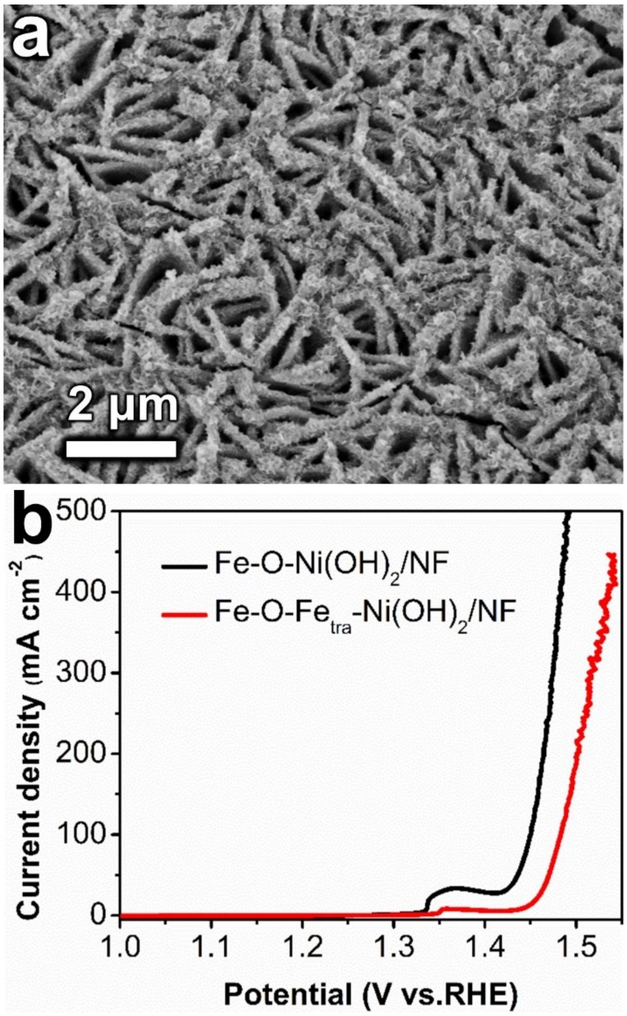

Figure S12. a) SEM images of Fe-O-Fe$_{tra}$-Ni(OH)$_2$/NF and b) LSV curves of Fe-O-Ni(OH)$_2$/NF and Fe-O-Fe$_{tra}$-Ni(OH)$_2$/NF.

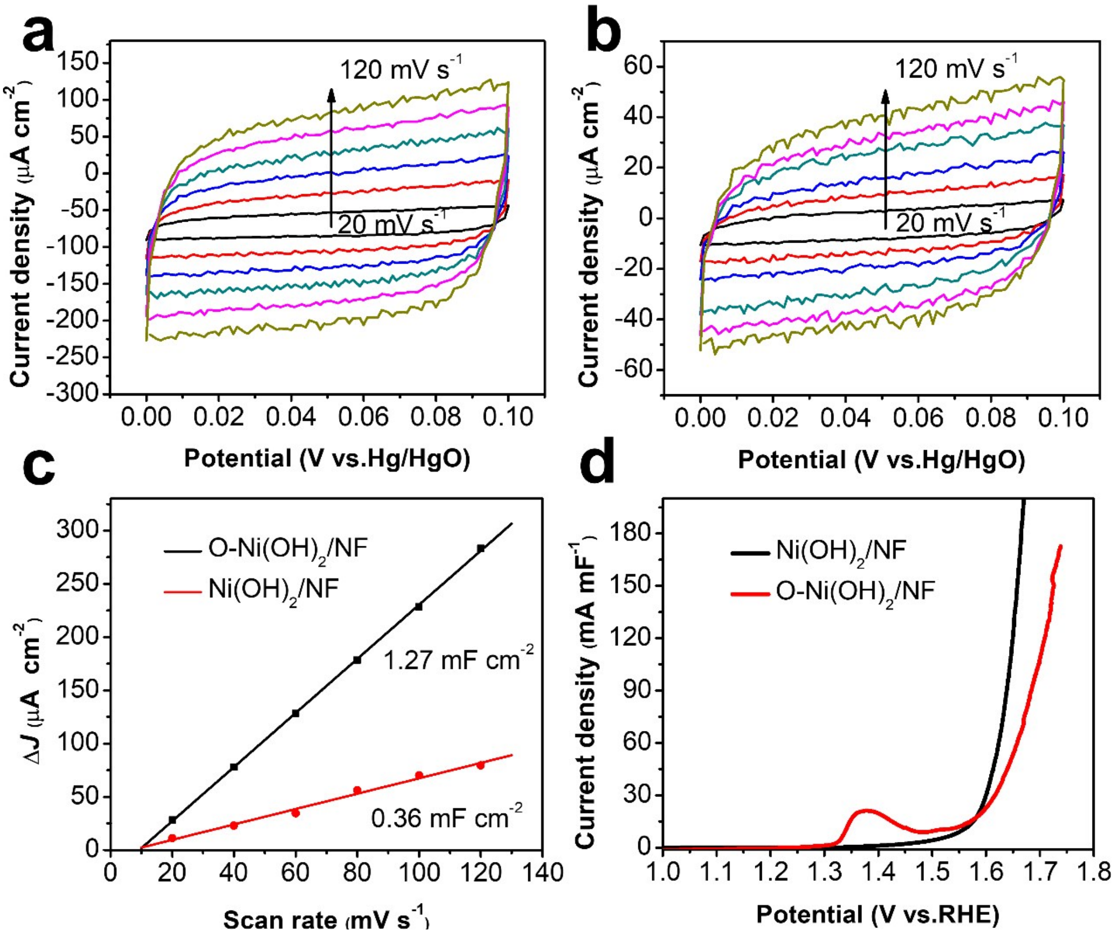

Figure S13. CV curves of a) O-$Ni(OH)_2$/NF and b) $Ni(OH)_2$/NF at the voltage between 0 and 0.1 V vs.Hg/HgO with different scan rates. c) Charging current density differences of O-$Ni(OH)_2$/NF and $Ni(OH)_2$/NF plotted against scan rates, double-layer capacitance (Cdl) is equivalent to a half of the linear slope. d) LSV curves of O-$Ni(OH)_2$/NF and $Ni(OH)_2$/NF normalized with respect to Cdl.

Table S1. Comparison of OER performance for Fe-O-Ni(OH)$_2$/NF with those of state-of-the-art electrocatalysts under alkaline conditions.

Material	Support	Loading (mg cm^{-2})	η @10 mA cm^{-2} (mV)	η @100 mA cm^{-2} (mV)	η @500 mA cm^{-2} (mV)	Reference
Fe-O-Ni(OH)$_2$	Ni foam	3	185	220	261	This work.
Ni:Pi-Fe	Ni foam	NA	220	NA	290	S1
$W_{0.5}Co_{0.4}Fe_{0.1}$	Ni foam	NA	250	300 @ 66.1 mA cm^{-2}	NA	S2
NiFeOx	Fe foam	NA	~225	~270	NA	S3
Fe:Ni(OH)2	Ni foam	NA	NA	~250	＞270	S4
a-NiFe-OH/NiFeP	Ni foam	2.1	199	NA	258 @ 300 mA cm^{-2}	S5
Gelled FeCoW	Au foam	0.21	190	NA	NA	S6
Ni_3FeN	Graphite carbon	0.35	280	~370	~670	S7
NiSe	Ni foam	2.8	270 @ 20 mA cm^{-2}	NA	370 @ ~350 mA cm^{-2}	S8
FeNi-rGO LDH	Ni foam	0.25	206	NA	NA	S9
$Ni_xFe_{1-x}Se_2$-DO	Ni foam	4.1	195	NA	262 @ ~250 mA cm^{-2}	S10
Nanoporous FexN	graphene/Ni foam	4	238	＞270	NA	S11
NiFeOx	Ni foam	NA	~226	260	NA	S12

Table S2. Comparison of OER performance for Fe-O-Ni(OH)$_2$/NF with those of state-of-the-art electrocatalysts under mild conditions.

Material	Support	Loading (mg cm^{-2})	Electrolyte	η @10 mA cm^{-2} (mV)	Reference
Fe-O-Ni$(OH)_2$	Ni foam	3	0.1 M $K_2B_4O_7$	324	This work.
NiFe-LDH@NiFe-Bi	Carbon cloth	2.3	0.1 M $K_2B_4O_7$	444	S13
Ni-Bi film	ITO	NA	0.1 M $K_2B_4O_7$	425 @ 1 mA cm^{-2}	18
CoP@Co-Bi-Pi	Ti	1.2	0.1 M $K_2B_4O_7$	410	S14
Co-Bi	Ti	NA	0.1 M $K_2B_4O_7$	469	S15
Ni-Bi	Carbon cloth	2.3	0.1 M $K_2B_4O_7$	470	S16
FeOOH	ITO	NA	0.5 M $K_2B_4O_7$	560	S17
Co_3O_4	Ti	0.147	1 M PBS	570 @ 23 mA cm^{-2}	S18
Co-Pi nanoarry	Ti	0.95	0.1 M PBS	450	S19

[S1] Y. Li and C. Zhao, *Chem. Mater.*, 2016, **28**, 5659-5666.

[S2] Y. Pi, Q. Shao, P. Wang, F. Lv, S. Guo, J. Guo and X. Huang, *Angew. Chem. Int. Ed.*, 2017, **129**, 4573-4577.

[S3] J. Wang, L. Ji, S. Zuo and Z. Chen, *Adv. Energy Mater.*, 2017, **7**, 1700107.

[S4] W. Zhang, J. Qi, K. Liu and R. Cao, *Adv. Energy Mater.*, 2016, **6**, 1502489.

[S5] H. Liang, A. N. Gandi, C. Xia, M. N. Hedhili, D. H. Anjum, U. Schwingenschlögl and H. N. Alshareef, *ACS Energy Lett.*, 2017, **2**, 1035-1042.

[S6] B. Zhang, X. Zheng, O. Voznyy, R. Comin, M. Bajdich, M. García-Melchor, L. Han, J. Xu, M. Liu, L. Zheng, F. P. G. d. Arquer, C. T. Dinh, F. Fan, M. Yuan, E. Yassitepe, N. Chen, T. Regier, P. Liu, Y. Li, P. D. Luna, A. Janmohamed, H. L. Xin, H. Yang, A. Vojvodic and E. H. Sargent, *Science*, 2016, **352**, 333-337.

[S7] X. Jia, Y. Zhao, G. Chen, L. Shang, R. Shi, X. Kang, G. I. N. Waterhouse, L.-Z. Wu, C.-H. Tung and T. Zhang, *Adv. Energy Mater.*, 2016, **6**, 1502585.

[S8] C. Tang, N. Cheng, Z. Pu, W. Xing and X. Sun, *Angew. Chem. Int. Ed.*, 2015, **54**, 9351-9355.

[S9] X. Long, J. Li, S. Xiao, K. Yan, Z. Wang, H. Chen and S. Yang, *Angew. Chem. Int. Ed.*, 2014, **53**, 7584-7588.

[S10] X. Xu, F. Song and X. Hu, *Nat. Commun.*, 2016, **7**, 12324.

[S11] F. Yu, H. Zhou, Z. Zhu, J. Sun, R. He, J. Bao, S. Chen and Z. Ren, *ACS Catal.*, 2017, **7**, 2052-2057.

[S12] J. Wang, L. Ji and Z. Chen, *ACS Catal.*, 2016, **6**, 6987-6992.

[S13] L. Yang, L. Xie, R. Ge, R. Kong, Z. Liu, G. Du, A. M. Asiri, Y. Yao and Y. Luo, *ACS Appl. Mater. Interfaces*, 2017, **9**, 19502-19506.

[S14] X. Sun, *ChemSusChem*, 2017, **10**, 1370-1374.

[S15] L. Yang, D. Liu, S. Hao, R. Kong, A. M. Asiri, C. Zhang and X. Sun, *J. Mater. Chem. A*, 2017, **5**, 7305-7308.

[S16] X. Ji, L. Cui, D. Liu, S. Hao, J. Liu, F. Qu, Y. Ma, G. Du, A. M. Asiri and X. Sun, *Chem. Commun.*, 2017, **53**, 3070-3073.

[S17] D. R. Chowdhury, L. Spiccia, S. S. Amritphale, A. Paul and A. Singh, *J. Mater. Chem. A*, 2016, **4**, 3655-3660.

[S18] J. J. Zhang, H. H. Wang, T. J. Zhao, K. X. Zhang, X. Wei, X. H. Li, S. I. Hirano and J. S. Chen, *ChemSusChem*, 2017, **10**, 2875-2879.

[S19] L. Xie, R. Zhang, L. Cui, D. Liu, S. Hao, Y. Ma, G. Du, A. M. Asiri and X. Sun, *Angew. Chem. Int. Ed.*, 2016, **129**, 1084-1088.